Available online at http://scik.org
Commun. Math. Biol. Neurosci. 2023, 2023:67
https://doi.org/10.28919/cmbn/7983
ISSN: 2052-2541

IMPACT OF SCREENING, TREATMENT, AND MISDIAGNOSE ON LYMPHATIC FILARIASIS TRANSMISSION: A MATHEMATICAL MODEL

IFFATRICIA HAURA FEBIRIANA, VANIA ADISAPUTRI, PUTRI ZAHRA KAMALIA, DIPO ALDILA*

Department of Mathematics, Faculty of Mathematics and Natural Sciences, Universitas Indonesia, Depok 16424, Indonesia

Abstract. A novel mathematical model is constructed in this article to understand the impact of active case findings and treatment to suppress the spread of lymphatic filariasis. The model is constructed as a nine-dimensional system of ordinary differential equations which considering the effect of misdiagnosis in the screening process. The analytical study was carried out to analyze the existence and stability of the equilibrium points, the control reproduction number, and the nonexistence of backward bifurcations in the model. Our analytical results show that the condition of free-filariasis will always be established if the control reproduction number is less than one. On the other hand, we always have a unique and stable endemic equilibrium if and only if the control reproduction number is greater than one. Our sensitivity analysis has shown that a combination of active case detection, duration, and successful probability of treatment could effectively reduce the intensity of lymphatic filariasis spread in the population.

Keywords: lymphatic filariasis; case detection; misdiagnose; equilibrium point; control reproduction number; bifurcation; sensitivity analysis; forward bifurcation.

2020 AMS Subject Classification: 00A69, 37N25, 93D20.

*Corresponding author
E-mail address: aldiladipo@sci.ui.ac.id
Received April 06, 2023

1. INTRODUCTION

Lymphatic filariasis is one of the world's oldest and most debilitating infectious diseases. This disease is the second largest cause of permanent and long-term disability in the world after mental disability [1]. In 1997, WHO designated lymphatic filariasis as a disease that had become a public health problem in the world. Lymphatic filariasis is indicated to have existed since 1500 BC [2]. The replica illustration indicates this in the funeral temple of Queen Hatshepsut, depicting the daughter of Punt suffering from elephantiasis in her legs. Later, photos of women with swelling in their lower legs and men with swelling in their scrotum around 1100–1200 AD were found in Japan [3].

After much research, microfilariae have been found in fluids in the scrotum, urine, blood, arms, lymph nodes, and the abdomen of mosquitoes. Furthermore, adult male filarial worms were discovered by Sibthrope. Furthermore, Shichiro Hida found adult male filarial worms in the left side of the seminiferous gland (the ducts in the male genital organs) in 1903 [3]. The case of lymphatic filariasis in Indonesia was first discovered in 1889 by Haga and Van Eecke in Jakarta, namely by finding sufferers of scrotal lymphatic filariasis. In 1937, Brug reported that filarial worms of the species that cause lymphatic filariasis in Indonesia are *Wuchereria bancrofti* and *Brugia malayi* [4].

In 2018, 51 million people worldwide were infected with lymphatic filariasis [5]. Meanwhile, in Indonesia, in 2018, there were 10,681 cases of lymphatic filariasis. Then, in 2019, lymphatic filariasis cases in Indonesia increased to 10,758 cases and spread across 34 provinces [6].

Lymphatic filariasis is included in vector-borne diseases. Vector-borne disease is a human disease caused by parasites and transmitted by vectors. Vectors are living organisms that can act as intermediaries between infectious pathogens and humans or animals [7]. Filariasis is a disease that attacks the ducts and lymph nodes, is caused by filarial worms, and is transmitted by mosquitoes [5]. Three species of worms cause lymphatic filariasis, namely *Wuchereria bancrofti*, *Brugia malayi*, and *Brugia timori* [5]. There are 23 species of mosquitoes from five genera, namely *Mansonia*, *Anopheles*, *Culex*, *Aedes*, and *Armigeres*, which are vectors of lymphatic filariasis [4].

The spread of lymphatic filariasis involves mosquitoes and humans. When a mosquito containing infective larvae (microfilaria stage 3) bites a human, the human will be infected with the microfilaria. Next, the infective larvae grow into adult worms, which can reproduce to produce new microfilariae. The collection of adult filarial worms can cause the flow of lymph gland secretions to become obstructed. Humans can transmit lymphatic filariasis to other humans through mosquitoes when the microfilariae are in the peripheral blood, and the human is already at the stage of acute infection [4].

There are three stages of lymphatic filariasis development: the incubation stage, the acute stage, and the chronic stage. During the incubation stage, the patient will not show any symptoms. Then, in the acute stage, clinical symptoms experienced by sufferers can include recurrent fever, headache, and feeling weak. As for the chronic stage, sufferers can experience swelling in several body parts, such as the legs, arms, and scrotum. If not handled properly, this disease can cause disability and psychosocial stigma, impacting the productivity of sufferers and decreasing their quality of life [4].

In lymphatic filariasis endemic areas, the majority of lymphatic filariasis sufferers do not show symptoms but are positive for microfilariae [4]. From this, the process of screening to determine whether there are microfilariae in a person's body is one of the efforts in controlling lymphatic filariasis. Screening is a process to identify someone who looks healthy but is at risk of contracting a disease so that early treatment can be carried out [8].

Each screening test kit has a different sensitivity and is not 100% accurate. The test kit will be stable if used before expiration and stored at the specified temperature [9]. So, its stability can be disturbed if the test kit is not stored at a fixed temperature or duration.

Based on studies from various countries, most of the test accuracy and consistency did not work as well as expected because the tests were carried out in various conditions by local technicians [10]. In Indonesia, inaccurate test results are caused by low-quality diagnostic test kits [11]. Furthermore, the antigen level is low enough that it cannot be detected, and the test results can produce false negatives in individuals [10]. It can be seen that in the screening process, there is a possibility of misdiagnosis. This can cause the undetected stage of human infection to become more severe, and the spread of lymphatic filariasis continues to occur.

Mathematical models have been used by many researchers to understand how diseases may spread among populations; please see [12, 13, 14, 15, 16, 17, 18, 19, 20] for some examples. In the lymphatic filariasis transmission model, there are several research models for the spread of lymphatic filariasis. The authors in [21] introduced a mathematical model for lymphatic filariasis transmission. In this model, they consider a delay in the infection period and conclude that focusing on early treatment is more important than late treatment. The authors in [22] consider a lymphatic filariasis transmission model with mass treatment after pre-testing intervention. A quarantine and treatment model for lymphatic filariasis was introduced by authors in [23]. Using sensitivity analysis, the authors conclude that mosquito mortality rates are the most sensitive parameter. In [24], the authors introduced mathematical models for lymphatic filariasis in Caraga Region, the Philippines. Using the Latin Hypercube Sampling (LHS) or Partial Rank Correlation Coefficient (PRCC) method, it was shown that the infected human population is most sensitive to treatment coverage (i.e., how much of the population receives treatment) and treatment rates (i.e., how effective the antifilarial drugs are in reducing the parasite density in infected humans). In [25], the authors consider the long-term effect of the medical treatment in lymphatic filariasis, and it is shown that the current medical treatment strategy will be able to reduce the long-term level of incidences. The authors in [26] consider the logistic growth in periodic environments of mosquitoes and model the transmission of lymphatic filariasis. The authors in [27] show that the effectiveness of the strategy to achieve filariasis control will be determined by successfully addressing two key factors: the need to maintain high community treatment coverages and the need to include vector control measures, especially in areas of high endemicity. Recently, the authors in [28] developed a filariasis model by considering two important factors, namely the treatment and bed-net use. Please see [29, 30, 31, 32] for more references on the mathematical model for filariasis transmission.

Based on the above description, we understand that early detection by screening is an important intervention to handle the rapid transmission of filariasis. However, not many mathematical models consider these factors. Furthermore, it is also possible that this screening failed to detect

filariasis in humans. Therefore, we introduce a novel mathematical model for filariasis transmission by considering some important factors, such as early screening, misdiagnosis, and the first and second doses of treatment.

The organization of the paper is as follows: We introduce our mathematical model in Section 2. Model analysis about the equilibrium points, control reproduction number, and local stability of equilibrium points are given in Section 3. Some numerical experiments are also provided in Section 3 to identify the impact of some crucial parameters on the control reproduction number. Lastly, we provide some discussion and conclusions in Section 4.

2. MODEL CONSTRUCTION

We construct our model in this section by considering some important factors, such as detected-undetected cases, symptomatic-asymptomatic cases, and active case findings. Let human and mosquito populations be divided based on their health conditions, as shown in Table 1. Hence, the total human population is given by

$$N_h(t) = S(t) + E(t) + E_t(t) + I_a(t) + I_t(t) + I_c(t) + R(t),$$

and for mosquito population given by $N_v(t) = U(t) + V(t)$.

TABLE 1. Description of variables used in System (1).

Variable	Description
$S(t)$	The number of susceptible humans for lymphatic filariasis at time t
$E(t)$	The number of undetected exposed individuals at time t
$E_t(t)$	The number of detected exposed individuals at time t
$I_a(t)$	The number of asymptomatic infected individuals at time t
$I_t(t)$	The number of symptomatic, detected, and treated infected individuals at time t
$I_c(t)$	The number of chronically infected individuals at time t
$R(t)$	The number of recovered individuals at time t
$U(t)$	The number of susceptible mosquitoes at time t
$V(t)$	The number of infected mosquitoes at time t
$N_h(t)$	The total human population at time t
$N_v(t)$	The total mosquito population at time t

The model construction process is based on Figure 1 and is described. We assume that the recruitment rate in the human and mosquito populations (Λ_h and Λ_v, respectively) is always born as a susceptible individuals. Infections in humans occur due to a successful bite from infected mosquitoes, with the average number of bites per day being θ_1 and the probability of a successful infection being β_1. We assume that infection with lymphatic filariasis in humans has an incubation period of δ_1^{-1}. Hence, we have the δ present transition rate from E to I_a due to the incubation of the filaria worm in the human body. We assume that an exposed individual cannot be detected without any testing. Hence, we assume that there is an effort by the government, with a rate of u, to conduct the lymphatic filariasis test, with a probability of humans being successfully detected is a. In our model, we assume that all exposed individuals will get an early treatment, which gives them a chance to be recovered with a probability of p after a treatment period of δ_2^{-1}. Exposed individuals who failed in treatment ($(1-p)E_t$) will go to the infected compartment and will get an advanced treatment. There is a transition from I_a to I_t due to the active finding with the lymphatic filariasis test. Without any treatment or detection, an infected individual in I_a will increase the infection status in I_c at a rate of η_a. Similar to treatment for E_t, we assume that treatment for I_t does not always eliminate lymphatic filariasis from I_t. Hence, after treatment duration η_t^{-1}, q proportion of I_t will be recovered, while $1-q$ will go to the chronic compartment I_c. We assume that the immunity from lymphatic filariasis is not permanent. Hence, there is a transition from R to S due to waning immunity.

Table 2: Description of parameters used in System 1.

Par	Description	Units	Value	Ref
Λ_h	Natural recruitment rate of the human population	$\frac{\text{human}}{\text{day}}$	$\frac{10000}{65\times365}$	Estimated
Λ_v	Natural recruitment rate of mosquitoes	$\frac{\text{mosquito}}{\text{day}}$	$\frac{10000}{21}$	Estimated
μ_h	Natural human death rate	$\frac{1}{\text{day}}$	$\frac{1}{65\times365}$	[22]
μ_v	Natural mosquito death rate	$\frac{1}{\text{day}}$	$\frac{1}{21}$	Estimated
β_1	The number of bites received by one human from one mosquito in one day	$\frac{\text{human}}{\text{mos}\times\text{day}}$	1	[22]

Continued on next page

Table 2: Description of parameters used in System 1. (Continued)

Par	Description	Units	Value	Ref
β_2	Biting rate of the mosquito to humans	$\frac{1}{\text{day}}$	1	[22]
θ_1	Probability of transmission success rate from mosquito to human	-	0.1	[31]
θ_2	Probability of transmission success rate from human to mosquito	-	0.1	Estimated
ω	Rate of loss of immunity in the recovered class	$\frac{1}{\text{day}}$	$\frac{1}{3}$	[31]
δ_1	Progression rate from exposed to acute class	$\frac{1}{\text{day}}$	$\frac{1}{4}$	[31]
δ_2	Treatment rate of the exposed totreatment class	$\frac{1}{\text{day}}$	$\frac{0.430848}{7}$	[24]
η_a	Progression rate from acute to chronic class	$\frac{1}{\text{day}}$	$\frac{1}{365}$	Estimated
η_t	Treatment rate of the acute-treatment class	$\frac{1}{\text{day}}$	0.1	Estimated
η_c	Treatment rate of the chronic class	$\frac{1}{\text{day}}$	0.1	Estimated
u	Screening rate	$\frac{1}{\text{day}}$	0.9	Estimated
a	Probability of humans being successfully detected	-	0.8	Estimated
ξ_t	Reducing factor for the number of microfilariae in the body of infected-acute humans due to treatment	-	0.8	Estimated
ξ_c	Reducing factor for the number of microfilariae in the body of chronically infected chronic humans due to treatment	-	0.0555	[23]
p	Successful probability of the first dose treatment	-	0.8	Estimated
q	Successful probability of the second dose treatment	-	0.9	[21]

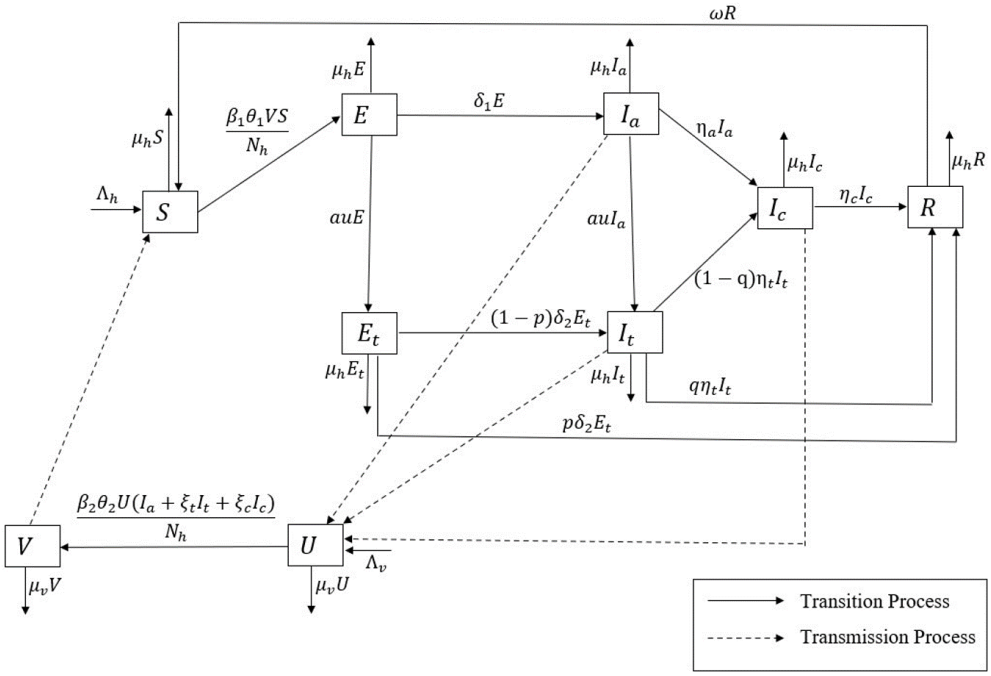

FIGURE 1. Transmission diagram of the lymphatic filariasis model in System (1).

Based on the transmission diagram in Figure 1 and the description of model derivations before, the mathematical model for malaria considering the changes in individual awareness is given by the following system of ordinary differential equations:

$$
\begin{aligned}
\frac{dS}{dt} &= \Lambda_h + \omega R - \frac{\beta_h VS}{N_h} - \mu_h S,\\
\frac{dE}{dt} &= \frac{\beta_h VS}{N_h} - (\alpha + \delta_1 + \mu_h)E,\\
\frac{dE_t}{dt} &= \alpha E - (\delta_2 + \mu_h)E_t,\\
\frac{dI_a}{dt} &= \delta_1 E - (\eta_a + \alpha + \mu_h)I_a,\\
\frac{dI_t}{dt} &= (1-p)\delta_2 E_t + \alpha I_a - (\eta_t + \mu_h)I_t,\\
\frac{dI_c}{dt} &= \eta_a I_a + (1-q)\eta_t I_t - (\eta_c + \mu_h)I_c,\\
\frac{dR}{dt} &= p\delta_2 E_t + q\eta_t I_t + \eta_c I_c - (\omega + \mu_h)R,\\
\frac{dU}{dt} &= \Lambda_v - \frac{\beta_v U(I_a + \xi_t I_t + \xi_c I_c)}{N_h} - \mu_v U,\\
\frac{dV}{dt} &= \frac{\beta_v U(I_a + \xi_t I_t + \xi_c I_c)}{N_h} - \mu_v V,
\end{aligned}
\tag{1}
$$

with $\alpha = au$, and the description of parameters can be seen in Table 2. This system is completed with non-negative initial conditions:

$$S(0) > 0, E(0) \geq 0, E_t(0) \geq 0, I_a(0) \geq 0, I_t(0) \geq 0,$$
$$I_c(0) \geq 0, R(0) \geq 0, U(0) \geq 0, V(0) \geq 0.$$

Using the same approach as the authors in [17, 33], we can show that our model always gives non-negative solutions for all $t > 0$.

3. Model Analysis

In this section, we analyze the existence criteria of all equilibrium points of System 1 and their relationship with the respective control reproduction number. A numerical experiment using our model was conducted using MATLAB.

3.1. Analytical results.

3.1.1. *The disease-free equilibrium.* The disease-free equilibrium point (DFE) is a condition where a disease is no longer present in a population. Based on this definition, the disease-free equilibrium point for the lymphatic filariasis spread model in System 1 is obtained when the solution to System 1 does not change over time, and the number of infected subpopulations is 0, both for the human and mosquito populations.

From this, we can find the values of S, R, and U by substituting $E = 0, E_t = 0, I_a = 0, I_t = 0, I_c = 0, V = 0$ into $\frac{dS}{dt} = 0, \frac{dR}{dt} = 0$, and $\frac{dV}{dt} = 0$. The disease-free equilibrium point of System 1 is given by

$$DFE = \left(S^0, E^0, E_t^0, I_a^0, I_t^0, I_c^0, R^0, U^0, V^0\right) = \left(\frac{\Lambda_h}{\mu_h}, 0, 0, 0, 0, 0, 0, 0, \frac{\Lambda_v}{\mu_v}, 0\right).$$

3.1.2. *The control reproduction number.* The control reproduction number is determined from the spectral radius of the next-generation matrix of the respective model. Using the next-generation matrix approach [34], the $\mathscr{R}_0$ of System 1 is given by,

$$\mathscr{R}_0 = \sqrt{\frac{\Lambda_h \Lambda_v \beta_h \beta_v k}{\mu_h \mu_v^2 N_h^2 (\eta_a + \alpha + \mu_h)(\alpha + \delta_1 + \mu_h)(\eta_t + \mu_h)(\delta_2 + \mu_h)(\eta_c + \mu_h)}}, \tag{2}$$

with k

$$k = (1-p)\left((1-q)\,\eta_t\xi_c + \xi_t\,(\mu_h+\eta_c)\right)\delta_2\alpha^2 + \left((1-q)\,\eta_t\xi_c + \xi_t\,(\mu_h+\eta_c)\right)$$
$$\left((\delta_2+\mu_h)\,\delta_1 + (1-p)\,\delta_2\,(\mu_h+\eta_a)\right)\alpha + \delta_1\,(\delta_2+\mu_h)\,(\mu_h+\eta_t)\,(\eta_a\xi_c+\eta_c+\mu_h).$$

To further interpret $\mathscr{R}_0$, the equation 2 can be rewritten as follows:

$$\mathscr{R}_0^2 = \underbrace{\left\{\frac{\beta_v}{\mu_v}\right\}}_{\text{In-out ratio Mos}}\underbrace{\left\{\frac{N_v}{N_h}\right\}}_{\text{Ratio human-mos}}\underbrace{\left\{\frac{1}{\eta_a+\alpha+mu_h}\right\}}_{\text{life time of } I_a}\underbrace{\left\{\frac{1}{\eta_t+mu_h}\right\}}_{\text{life time of } I_t}\underbrace{\left\{\frac{1}{\eta_c+mu_h}\right\}}_{\text{life time of } I_c}$$
$$\underbrace{\left\{\frac{\beta_h}{\alpha+\delta_1+\mu_h}\right\}}_{\text{life time of } E}\underbrace{\left\{\frac{1}{\delta_2+mu_h}\right\}}_{\text{life time of } E_t}k$$

It is clearly observed that $\mathscr{R}_0$ is a result of the multiplication of the number of newly infected humans, newly infected mosquitoes, a lifetime of infected and detected exposed human compartments, and k. Furthermore, it is easy to show that System 1 satisfies the five conditions in van den Driessche's theorem [35]. Hence, using the result in [35], the local stability criteria of DFE are stated in the following theorem.

Theorem 3.1. *The disease-free equilibrium of System 1 (DFE) is always locally asymptotically stable if* $\mathscr{R}_0 < 1$ *and unstable if* $\mathscr{R}_0 > 1$.

In a special case where there is no intervention (case detection and treatment), we have that $\alpha = \delta_2 = \eta_t = p = q = 0$. Hence, the basic reproduction number of model 1 is given by $\mathscr{R}_0^*$ as follows:

$$\mathscr{R}_0^* = \sqrt{\frac{\beta_h\Lambda_h\beta_v\Lambda_v\delta_1\,(\xi_c\eta_a+\eta_c+\mu_h)}{\mu_h{N_h}^2{\mu_v}^2\,(\delta_1+\mu_h)\,(\eta_a+\mu_h)\,(\eta_c+\mu_h)}}. \tag{3}$$

To further interpret $\mathscr{R}_0$, the equation 3 can be rewritten as follows:

$$\mathscr{R}_0^{*^2} = \underbrace{\left\{\frac{\beta_v}{\mu_v}\right\}}_{\text{In-out ratio Mos}}\underbrace{\left\{\frac{\beta_h}{\delta_1+\mu_h}\right\}}_{\text{In-out ratio Human}}\underbrace{\left\{\frac{N_v}{N_h}\right\}}_{\text{Ratio human-mos}}\underbrace{\left\{\frac{\delta_1}{\eta_a+mu_h}\right\}}_{\text{life time of } E}\underbrace{\left\{\frac{\xi_c\eta_a+\eta_c+\mu_h}{\eta_c+mu_h}\right\}}_{\text{life time of } I_c}.$$

It can be seen if there is no intervention (case detection and treatment), we have that $\mathscr{R}_0 < \mathscr{R}_0^*$.

3.1.3. *Endemic equilibrium.* The endemic equilibrium point (EE) is interpreted as a condition when a disease is always present in a population. Based on this definition, the endemic equilibrium point for System 1 is obtained when the solution of System 1 does not change with time and when the number of infected individuals is not equal to zero ($E \neq 0, E_t \neq 0, I_a \neq 0, I_t \neq 0, I_c \neq 0, V \neq 0$).

From this, we can find the values of $S, E, E_t, I_a, I_t, I_c, R, U$ and V that satisfy

$$\frac{dS}{dt} = 0, \frac{dE}{dt} = 0, \frac{dE_t}{dt} = 0, \frac{dI_a}{dt} = 0, \frac{dI_t}{dt} = 0, \frac{dI_c}{dt} = 0, \frac{dR}{dt} = 0, \frac{dU}{dt} = 0, \frac{dV}{dt} = 0$$

The endemic equilibrium point of System 1 is given by

$$EE = (S^*, E^*, E_t^*, I_a^*, I_t^*, I_c^*, R^*, U^*, V^*),$$

where

$$\begin{aligned}
S^* &= \frac{E_t^* N_h (\mu_h + \delta_2)(\mu_h + \alpha + \delta_1)}{V^* \alpha \beta_h}, \\
E^* &= \frac{E_t^* (\delta_2 + \mu_h)}{\alpha}, \quad E_t^* = \frac{M_0}{M_1}, \quad I_a^* = \frac{E_t^* \delta_1 (\delta_2 + \mu_h)}{\alpha(\eta_a + \alpha + \mu_h)}, \\
I_t^* &= \frac{E_t^* (\alpha\delta_2(1-p) + \delta_2\eta_a(1-p) + \delta_2\mu_h(1-p) + \delta_1\delta_2 + \delta_1\mu_h}{(\eta_t + \mu_h)(\alpha + \eta_a + \mu_h)}, \\
I_c^* &= \frac{E_t^* M_2}{\alpha(\eta_c + \mu_h)(\eta_t + \mu_h)(\alpha + \eta_a + \mu_h)}, \\
R^* &= \frac{M_3}{\beta_h \alpha V^* \omega}, \quad U^* = \frac{\Lambda_v}{\mu_v} - V^*,
\end{aligned}$$

with

$$\begin{aligned}
M_0 &= V^* \alpha N_h \mu_v (\eta_t + \mu_h)(\eta_c + \mu_h)(\alpha + \eta_a + \mu_h), \\
M_1 &= U^* \beta_v (\delta_1 (\mu_h + \delta_2)((1-q)\eta_t \xi_c + \xi_t (\mu_h + \eta_c)) + \delta_2 \alpha (\alpha + \mu_h + \eta_a) \\
&\quad ((1-p)(1-q)\eta_t \xi_c + (1-p)\xi_t (\mu_h + \eta_c)), \\
M_2 &= (\mu_h + \delta_2)((\mu_h + \eta_t)\eta_a + \alpha\eta_t (1-q))\delta_1 + \alpha\delta_2\eta_t (1-q)(1-p)(\alpha + \eta_a + \mu_h), \\
M_3 &= V^* E_t^* ((\eta_2 + \mu_h)\alpha + (\mu_h + \delta_2)(\mu_h + \delta_1))(\beta_h + N_h\mu_h) - V^* \alpha \Lambda_h \beta_h.
\end{aligned}$$

To have a biological meaning, R^* and U^* must be positive, so $M_3 > 0$ and $-V^* + \frac{\Lambda_v}{\mu_v} > 0$ or in other words,

$$V^*E_t^*((\eta_2+\mu_h)\,\alpha+(\mu_h+\delta_2)\,(\mu_h+\delta_1))(\beta_h+N_h\mu_h) > V^*\alpha\Lambda_h\beta_h \text{ and } V^* < \frac{\Lambda_v}{\mu_v}.$$

We know that V^* is a positive solution of the following linear equation:

$$a_1V^*+a_0=0, \tag{4}$$

with

$$a_0=(\omega+\mu_h)(\eta_t+\mu_h)(\eta_c+\mu_h)(\delta_2+\mu_h)(\eta_a+\alpha+\mu_h)(\alpha+\delta_1+\mu_h)N_h^2\mu_h\mu_v^2(1+\mathscr{R}_0)(1-\mathscr{R}_0),$$

where a_1 has a long expression to be shown in this article. However, we can confirm that a_1 is always positive. From the expression of a_0 and since a_1 is always positive, we have the following theorem:

Theorem 3.2. *System 1 has a unique endemic equilibrium if and only if $\mathscr{R}_0 > 1$ and has no endemic equilibrium otherwise.*

3.1.4. *Bifurcation analysis.* In this section, we continue our analysis of the stability of the lymphatic filariasis endemic equilibrium from the previous section. From Theorem 3.2, we know that the endemic equilibrium is unique and only appears when $\mathscr{R}_0 > 1$. To analyze the local stability of the endemic equilibrium, we will use the bifurcation theorem introduced by Castillo and Song in [36]. Let us assume

$$S=y_1,\ E=y_2,\ E_t=y_3,\ I_a=y_4,\ I_t=y_5,\ I_c=y_6,\ R=y_7,\ U=y_8,\ V=y_9.$$

Hence, System 1 can be written as

$$\begin{aligned}
g_1 &:= \frac{dy_1}{dt} = \Lambda_h+\omega y_7-\frac{\beta_h y_9 y_1}{N_h}-\mu_h y_1,\\
g_2 &:= \frac{dy_2}{dt} = \frac{\beta_h y_9 y_1}{N_h}-(\alpha+\delta_1+\mu_h)y_2,\\
g_3 &:= \frac{dy_3}{dt} = \alpha y_2-(\delta_2+\mu_h)y_3,\\
g_4 &:= \frac{dy_4}{dt} = \delta_1 y_2-(\eta_a+\alpha+\mu_h)y_4,\\
g_5 &:= \frac{dy_5}{dt} = (1-p)\delta_2 y_3+\alpha y_4-(\eta_t+\mu_h)y_5,
\end{aligned} \tag{5}$$

$$g_6 := \frac{dy_6}{dt} = \eta_a y_4 + (1-q)\eta_t y_5 - (\eta_c + \mu_h) y_6,$$
$$g_7 := \frac{dy_7}{dt} = p\delta_2 y_3 + q\eta_t y_5 + \eta_c y_6 - (\omega + \mu_h) y_7,$$
$$g_8 := \frac{dy_8}{dt} = \Lambda_v - \frac{\beta_v y_8 (y_4 + \xi_t y_5 + \xi_c y_6)}{N_h} - \mu_v y_8,$$
$$g_9 := \frac{dy_9}{dt} = \frac{\beta_v y_8 (y_4 + \xi_t y_5 + \xi_c y_6)}{N_h} - \mu_v y_9.$$

We assumed $\beta_h^* = \frac{B_0}{B_1}$ (please see Appendix 1 for definitions of B_0 and B_1) as the bifurcation parameter such that the critical value of β_h^* makes $\mathscr{R}_0 = 1$. The linearized System 5 at β_h^* yields,

$$\mathbf{J} = \begin{bmatrix} -\mu_h & 0 & 0 & 0 & 0 & 0 & \omega & 0 & a_{19} \\ 0 & a_{22} & 0 & 0 & 0 & 0 & 0 & 0 & a_{29} \\ 0 & \alpha & a_{33} & 0 & 0 & 0 & 0 & 0 & 0 \\ 0 & \delta_1 & 0 & a_{44} & 0 & 0 & 0 & 0 & 0 \\ 0 & 0 & a_{53} & \alpha & a_{55} & 0 & 0 & 0 & 0 \\ 0 & 0 & 0 & \eta_a & a_{65} & a_{66} & 0 & 0 & 0 \\ 0 & 0 & p\delta_2 & 0 & q\eta_t & \eta_c & a_{77} & 0 & 0 \\ 0 & 0 & 0 & -\frac{\Lambda_v \beta_v}{\mu_v N_h} & -\frac{\Lambda_v \beta_v \xi_t}{\mu_v N_h} & -\frac{\Lambda_v \beta_v \xi_c}{\mu_v N_h} & 0 & -\mu_v & 0 \\ 0 & 0 & 0 & \frac{\Lambda_v \beta_v}{\mu_v N_h} & \frac{\Lambda_v \beta_v \xi_t}{\mu_v N_h} & \frac{\Lambda_v \beta_v \xi_c}{\mu_v N_h} & 0 & 0 & -\mu_v \end{bmatrix},$$

with

$$a_{19} = \frac{p_1}{p_2},\ \ a_{22} = -\alpha - \delta_1 - \mu_h,\ \ a_{29} = \frac{q_1}{q_2},\ \ a_{33} = -\delta_2 - \mu_h,\ \ a_{44} = -\eta_a - \alpha - \mu_h,$$
$$a_{53} = (1-p)\delta_2,\ \ a_{55} = -\eta_t - \mu_h,\ \ a_{65} = (1-q)\eta_t,\ \ a_{66} = -\eta_c - \mu_h,\ \ a_{77} = -\omega - \mu_h,$$

and please see Appendix 2 for p_1, p_2, q_1, q_2. The characteristic polynomial of $\mathscr{A}$ is given by,

$$\lambda(\lambda + \mu_v)(\lambda + \omega + \mu_h)(\lambda + \mu_h)(c_0\lambda^5 + c_1\lambda^4 + c_2\lambda^3 + c_3\lambda^2 + c_4\lambda + c_5) = 0.$$

Where c_i for $i = 1, 2, ..., 5$, are positive (which has a long-expression to show in this article). Hence, we have a simple zero eigenvalue, and the other eigenvalues are negative. Next, we

calculated the right eigenvectors of $\mathscr{A}$, denoted by $\mathbf{w} = (w_1, w_2, ..., w_9)^T$, which satisfies $\mathscr{A}\mathbf{w} = 0$. Please see Appendix 3 for the expression of $\mathbf{w}$. Now, we have the left eigenvectors of $\mathscr{A}$, denoted by $\mathbf{v} = (v_1, v_2, ..., v_9)$, which satisfies $\mathbf{v}\mathscr{A} = 0$. Please see Appendix 4 for the expression of $\mathbf{v}$.

Since we have:

(1) Zero is a simple eigenvalue of the linearization matrix of the system around the disease-free equilibrium with $\mathscr{R}_0$ evaluated at disease-free equilibrium, and

(2) This linearization matrix has a non-negative right and left eigenvector, where each corresponds to the zero eigenvalue, and other eigenvalues have negative real parts.

Then, our system can be analyzed using Castillo and Song [36].

To use the Castillo-Chavez and Song theorem, we calculated the values of $\mathbf{J}$ as follows:

$$\begin{aligned}
\mathscr{A} &= \sum_{k,i,j=1}^{9} v_k w_i w_j \frac{\partial^2 g_k}{\partial y_i \partial y_j}(0,0) \\
&= v_2 w_1 w_9 \frac{\partial g_2}{\partial y_1 \partial y_9}(0,0) + v_2 w_9 w_1 \frac{\partial g_2}{\partial y_9 \partial y_1}(0,0) + v_9 w_4 w_8 \frac{\partial g_9}{\partial y_4 \partial y_8}(0,0) \\
&+ v_9 w_5 w_8 \frac{\partial g_9}{\partial y_5 \partial y_8}(0,0) + v_9 w_6 w_8 \frac{\partial g_9}{\partial y_6 \partial y_8}(0,0) + v_9 w_8 w_4 \frac{\partial g_9}{\partial y_8 \partial y_4}(0,0) \\
&+ v_9 w_8 w_5 \frac{\partial g_9}{\partial y_8 \partial y_5}(0,0) + v_9 w_8 w_6 \frac{\partial g_9}{\partial y_8 \partial y_6}(0,0) \\
&= v_2 w_1 w_9 \left(\frac{2\beta_h^*}{N_h}\right) + v_9 w_4 w_8 \left(\frac{2\beta_v}{N_h}\right) + v_9 w_5 w_8 \left(\frac{2\beta_v \xi_t}{N_h}\right) + v_9 w_6 w_8 \left(\frac{2\beta_v \xi_c}{N_h}\right).
\end{aligned}$$

From Appendices 3 and 4, we have $w_1 < 0, w_4 > 0, w_5 > 0, w_6 > 0, w_8 < 0, w_9 > 0, v_2 > 0$, and $v_9 > 0$. We know that $N_h > 0$, $\beta_h^* > 0$, and other parameters are positive. Hence, $\mathscr{A} < 0$.

Next, we calculate $\mathscr{B}$ as follows:

$$\mathscr{B} = \sum_{k,i=1}^{9} v_k w_i \frac{\partial^2 g_k}{\partial y_i \partial \beta_h}(0,0) = v_2 w_9 \frac{\partial^2 g_2}{\partial y_9 \partial \beta_h}(0,0) = v_2 w_9 \frac{\Lambda_h}{\mu_h N_h}.$$

From Appendices 3 and 4, we have $w_9 > 0$ and $v_2 > 0$. We know that $N_h > 0, \Lambda_h > 0$, and $\mu_h > 0$. Hence, $\mathscr{B} > 0$.

According to these results, the following theorem is obtained:

Theorem 3.3. *The lymphatic filariasis endemic equilibrium of System 1 (EE) is always locally asymptotically stable if $\mathscr{R}_0 > 1$, but close to one.*

3.2. Results of the numerical experiment.

3.2.1. *Visualization of stability theorem.* For the first simulation, we show the impact of case detection on the size of $\mathscr{R}_0$ and the endemic equilibrium of infected mosquitoes. To conduct this simulation, we substitute all parameter values as shown in Table 2 except α, which is set to be the independent parameter in the expression of $\mathscr{R}_0$ in equation (2) and the endemic equilibrium of V, which is the solution of equation (4) with respect to V. The result is given in Figure 2. We can see how the increases in case detection success reduce $\mathscr{R}_0$ and the endemic equilibrium of V. The endemic equilibrium size of V is significantly decreasing until it reaches point P_1, where $\mathscr{R}_0 = 1$. P_0 is the point where α makes $\mathscr{R}_0 = 1$. According to Theorem 3.3, the endemic equilibrium disappears when α increases more than P_1, which makes $\mathscr{R}_0$ become smaller than one.

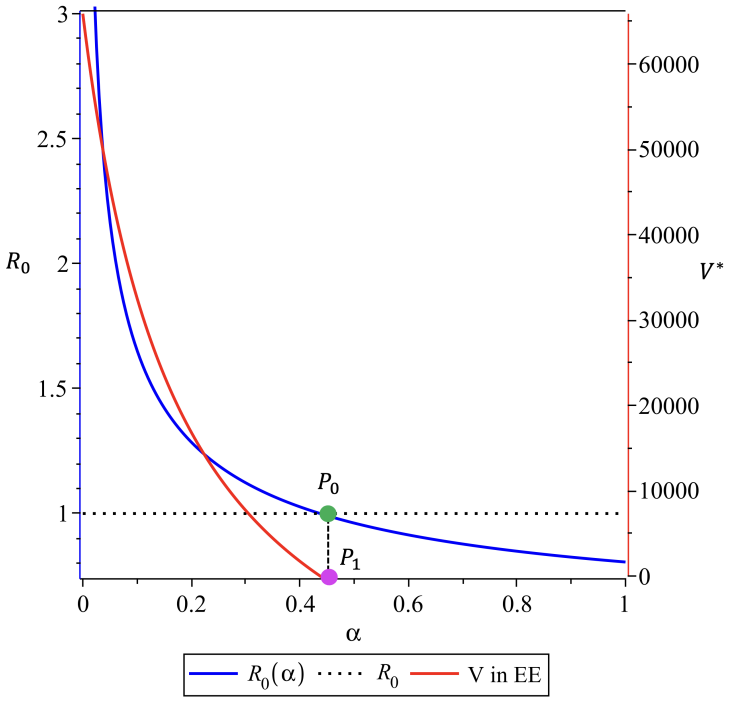

FIGURE 2. Impact of case detection (α) on the size of $\mathscr{R}_0$ (blue curve) and infected mosquitoes at endemic equilibrium (red curve). All parameter values are in Table 2, except α, which is set as an independent parameter.

Next, we visualize Theorems 3.1 and 3.3 using numerical simulations. For the case of $\mathscr{R}_0 = 1.12 > 1$, the rate value of screening was used, which was successful in detecting microfilariae

($\alpha = 0.3$), and other parameter values refer to Table 2. In the case of $\mathscr{R}_0 = 0.99 < 1$, the value of $\alpha = 0.45$ is used, and the other parameter values refer to Table 2. Each of these conditions is simulated with different initial values. The following is a graph of these conditions.

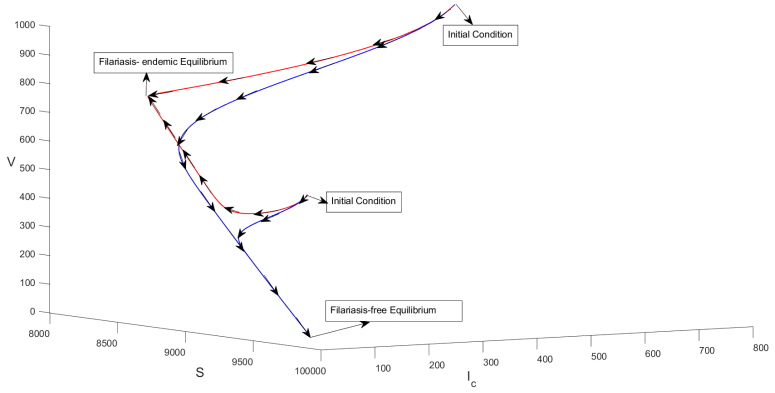

FIGURE 3. The trajectories of $S(t), I_c(t)$, and $V(t)$ for several initial conditions tend to a stable disease-free (blue) and endemic (red) equilibrium point.

In Figure 3, the red graph depicts when condition $\mathscr{R}_0 > 1$, and the blue graph depicts when condition $\mathscr{R}_0 < 1$. When $\mathscr{R}_0 > 1$, it can be seen that all solutions tend to the same endemic equilibrium point. The endemic equilibrium point given by $EE = (S^* = 8,587, E^* = 120.17, E_t^* = 585.34, I_a^* = 99.22, I_t^* = 369.57, I_c^* = 39.66, R^* = 198.12, U^* = 9,230, V^* = 769.69)$. On the other hand, when $\mathscr{R}_0 < 1$, it can be seen that all solutions tend to the same disease-free equilibrium point. The disease-free equilibrium point given by $DFE = (S^0 = 10,000, E^0 = 0, E_t^0 = 0, I_a^0 = 0, I_t^0 = 0, I_c^0 = 0, R^0 = 0, U^0 = 10,000, V^0 = 0)$. From this, it can be seen that with different initial values, the system will go to the same equilibrium point. This figure confirms Theorem 3.1 and Theorem 3.3.

3.2.2. *Normalize sensitivity analysis.* To know the impact on $\mathscr{R}_0$, we conducted the elasticity analysis of every parameter to $\mathscr{R}_0$ using the formula (6), where P is a parameter. The formula for calculating the elasticity of $\mathscr{R}_0$ is defined as follows [37]:

$$\varepsilon_{\mathscr{R}_0}^P = \frac{\partial \mathscr{R}_0}{\partial P} . \frac{P}{\mathscr{R}_0} \approx \frac{\%\Delta \mathscr{R}_0}{\%\Delta P} \tag{6}$$

To find out the value of this elasticity, look at two cases, namely $\mathscr{R}_0 < 1$ and $\mathscr{R}_0 > 1$. For cases $\mathscr{R}_0 < 1$, we used the parameter values listed in Table 2. In this case, the resulting $\mathscr{R}_0$

value is $0.87 < 1$. Meanwhile, for the case of $\mathscr{R}_0 > 1$, the value of the screening rate parameter, which successfully detected microfilariae $\alpha = 0.18$, was used, and the other parameter values are shown in Table 2. In this case, the resulting $\mathscr{R}_0$ value was $1.33 > 1$. Figures 4 and 5 show the tornado diagram for the cases of $\mathscr{R}_0 < 1$ and $\mathscr{R}_0 > 1$, respectively.

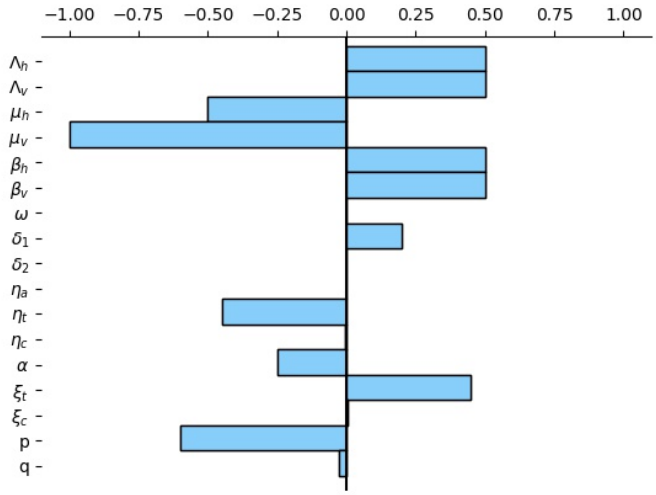

FIGURE 4. Normalize the sensitivity of $\mathscr{R}_0$ with respect to all parameter values for a condition of $\mathscr{R}_0 < 1$.

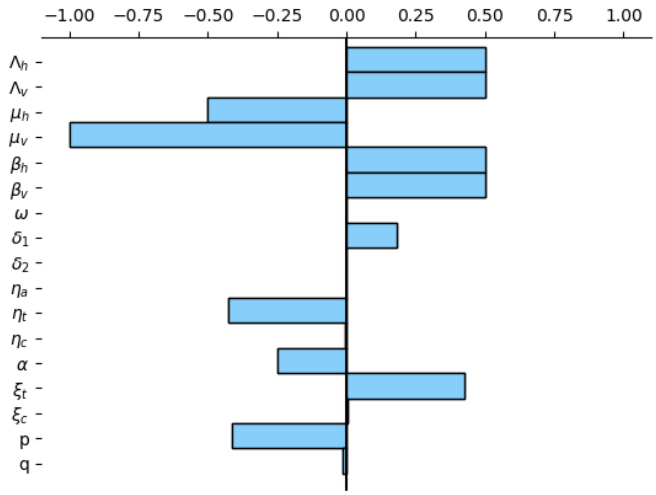

FIGURE 5. Normalize the sensitivity of $\mathscr{R}_0$ with respect to all parameter values for a condition of $\mathscr{R}_0 > 1$.

For $\mathscr{R}_0 < 1$, we can see that the most significant parameter in $\mathscr{R}_0$ is μ_v, followed by $p, \mu_h, \Lambda_h, \Lambda_v, \beta_h, \beta_v, \xi_t, \eta_t, \alpha, \delta_1, q, \xi_c, \eta_c, \eta_a, \delta_2$ and ω. Meanwhile, for $\mathscr{R}_0 > 1$, we can see that the most significant parameter in $\mathscr{R}_0$ is μ_v, followed by $\mu_h, \Lambda_h, \Lambda_v, \beta_h, \beta_v, \alpha, \xi_t, \eta_t, \delta_1, p, q, \eta_a$, ξ_c, η_c, δ_2, and ω. Therefore, it can be seen that $\mathscr{R}_0$ increases when $\Lambda_h, \Lambda_v, \beta_h, \beta_v, \delta_1, \delta_2, \xi_t$, or ξ_c increases. In contrast, increasing the value of $\mu_h, \mu_v, \eta_a, \eta_t, \eta_c, \alpha, p$, or q will reduce $\mathscr{R}_0$. It can be seen that $\varepsilon_\omega^{\mathscr{R}_0} = 0$, which means that the rate loss immunity does not influence the magnitude of $\mathscr{R}_0$.

3.2.3. *Autonomous simulation.* We conducted autonomous simulations to understand the effect of the intervention on several parameters related to the spread of lymphatic filariasis. We use the parameter values, as shown in Table 2, and the initial condition $S(0) = 9,500, E(0) = 100, E_t(0) = 0, I_a(0) = 100, I_t(0) = 0, I_c(0) = 100, R(0) = 200, U(0) = 9,500, V(0) = 500$. This simulation was carried out using the Runge-Kutta method of order four-five [36] with the help of MATLAB. The time observed in this simulation is 1500 days.

(1) Effects of case detection (α) and second treatment duration (η_t) on $\mathscr{R}_0$ and the dynamics of the infected population.

We analyzed the impacts of case detection (α) and second treatment duration (η_t) on $\mathscr{R}_0$ by defining $\mathscr{R}_0$ as a function of η_t and α. Hence, we have $\mathscr{R}_0 := \mathscr{R}_0(\eta_t, \alpha)$ as follows:

$$\mathscr{R}_0 = 5,84 \sqrt{\frac{h_2(\alpha, \eta_t)}{\left(\eta_t + \frac{1}{23.73}\right)(\alpha + 0.25)\left(\frac{66}{23.73} + \alpha\right)}},$$

with

$$h_2(\alpha, \eta_t) = 0.000068\alpha^2\eta_t + 0.00099\alpha^2 + 0.000086\alpha\eta_t$$
$$+ 0.00124\alpha + 0.0015\eta_t + 6.50 \times 10^{-8}.$$

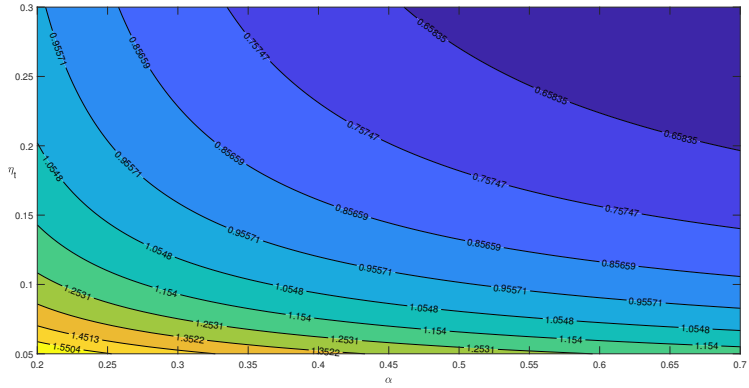

FIGURE 6. Sensitivity of α and η_t to the level set of $\mathscr{R}_0$.

As shown in Figure 6, it can be seen that the greater the value of the parameter α, the value of $\mathscr{R}_0$ gets smaller. Then, it is also seen that the greater the value of the parameter η_t, the smaller the value of $\mathscr{R}_0$. This confirms the elasticity value that was previously obtained.

a. Variation of α The next simulation was carried out with a variation of the case detection parameter (α). We used four values of α. First value using α from parameter estimation ($\alpha = 0.30$). The second, third, and fourth values were the values when we increased the case detection $(\alpha = 0.35, \alpha = 0.40, \alpha = 0.45)$. The results are shown in Figure 7.

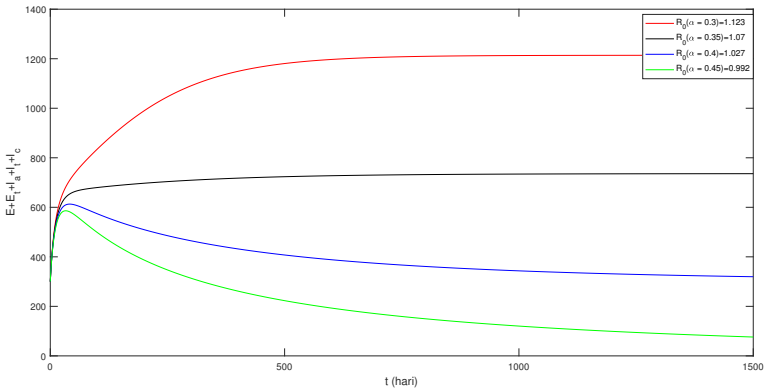

FIGURE 7. The dynamic of total infected humans for various values of α.

As you can see in Figure 7, when we increased the case detection, the number of infected humans decreased. So increasing the case detection rate is effective in reducing the number of infected humans in the population.

b. Variation of η_t The next simulation was carried out with a variation of the second treatment duration parameter (η_t). We used four values of η_t. First value using η_t from parameter estimation ($\eta_t = 0.073$). The second, third, and fourth values were the values when we increased the second treatment duration ($\eta_t = 0.078, \eta_t = 0.083, \eta_t = 0.088$). The results are shown in Figure 8.

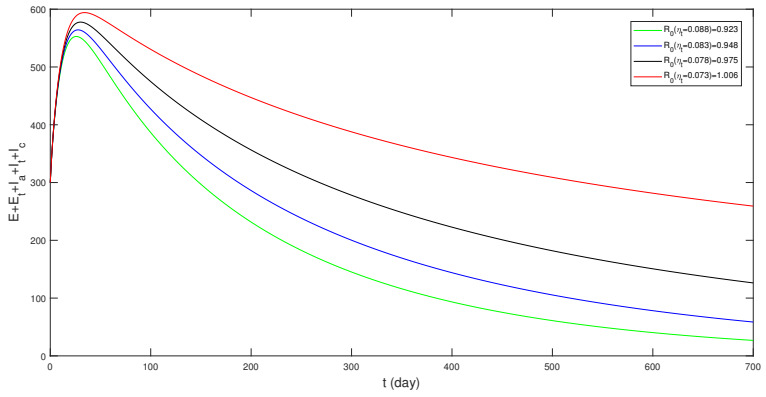

FIGURE 8. The dynamic of total infected humans for various values of η_t.

As you can see in Figure 8, when we increased the second treatment duration, the number of infected humans decreased. So increasing the second treatment duration is effective in reducing the number of infected humans in the population.

(2) Effects of the proportion of acutely infected humans that consume the drug regularly (p) and the proportion of chronically infected humans that consume the drug regularly (q) on $\mathscr{R}_0$ and the dynamics of the infected population.

We analyzed the impacts of the proportion of acutely infected humans that consume the drug regularly (p) and the proportion of chronically infected humans that consume the drug regularly (q) on $\mathscr{R}_0$ by defining $\mathscr{R}_0$ as a function of p and q. Hence, we have $\mathscr{R}_0 := \mathscr{R}_0(p,q)$ as follows:

$$\mathscr{R}_0 = \sqrt{0.86 - 0.61p + 282.28(0.004pq - 0.004p - 0.005q + 0.005)^2}$$

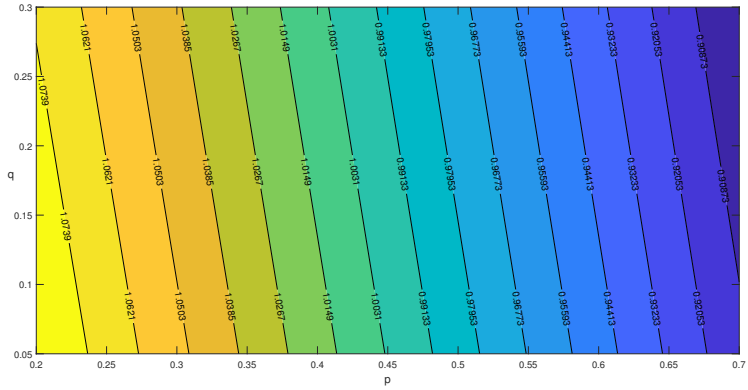

FIGURE 9. Sensitivity of p and q to the level set by $\mathscr{R}_0$.

As shown in Figure 9, it can be seen that as the parameter p is increased, the value of $\mathscr{R}_0$ decreases. Then, it is also seen that the greater the value of the parameter q, the smaller the value of $\mathscr{R}_0$. This confirms the elasticity value that was previously obtained.

a. Variation of p The next simulation was carried out with a variation in the proportion of infected-acute humans that consume the drug regularly (p). We used four values of p. The first value using $p = 0.97$. The second, third, and fourth values were the values when we decreased the proportion $(p = 0.9, p = 0.5, p = 0.1)$. The results are shown in Figure 10.

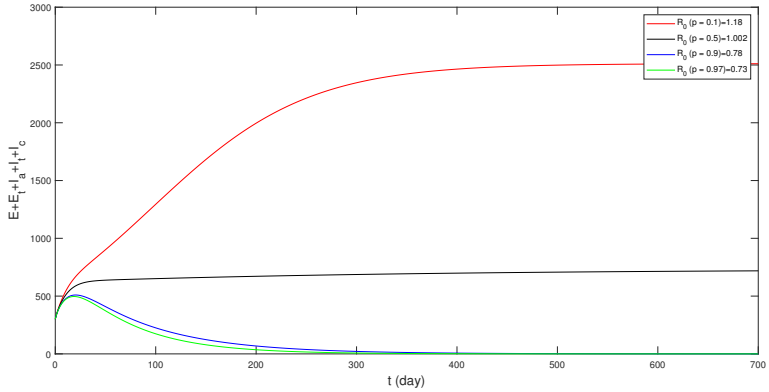

FIGURE 10. The dynamic of total infected humans for various values of p.

As you can see in Figure 10, when we decreased the proportion of infected-acute humans who consumed the drug regularly, the number of infected humans increased. So increasing the proportion of infected-acute humans that consume the drug regularly is effective in reducing the number of infected humans in the population.

b. Variation of q The next simulation was carried out with a variation in the proportion of infected-chronic humans that consume the drug regularly (q). We used four values of q. The first value using $q = 0.01$. The second, third, and fourth values were the values when we increased the proportion $(q = 0.1, q = 0.5, q = 0.9)$. The results are shown in Figure 11.

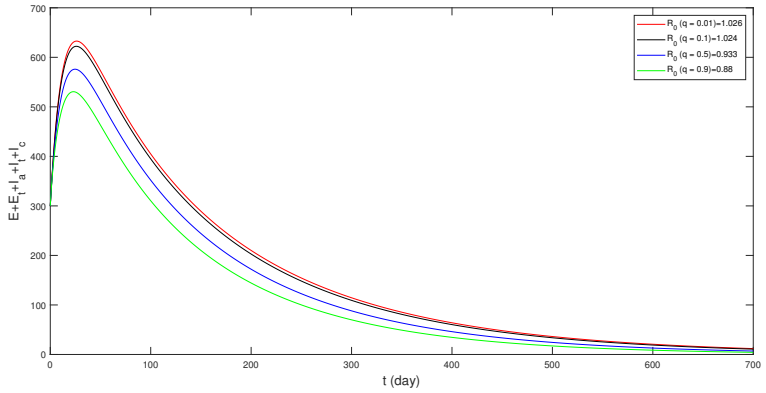

FIGURE 11. The dynamic of total infected humans for various values of q.

As you can see in Figure 11, when we increased the proportion of chronically infected humans who consumed the drug regularly, the number of infected humans decreased. So increasing the proportion infected-chronic human that consume the drug regularly is effective in reducing the number of infected humans in the population.

4. CONCLUSIONS

Vector-borne diseases have been found in many tropical and sub-tropical countries, such as malaria, dengue, lymphatic filariasis, chikungunya, etc. Filariasis is a vector-borne disease in which infected individuals have the opportunity to experience lifelong disabilities, such as permanent swelling in several parts of the body [5]. Various interventions have been implemented

in many countries, such as case detection and intensive interventions [38], [39], and [40]. Therefore, we proposed a mathematical model for lymphatic filariasis transmission in this article. We consider the impact of case detection (screening), treatment, and possible misdiagnosis phenomena on our model.

We discussed the existence and local stability equilibrium of our model. The first equilibrium is the filariasis-free equilibrium, which is locally asymptotically stable if the control reproduction number is less than one. The filariasis-endemic equilibrium point only exists (and is unique) if the control reproduction number is greater than one. Using the Castillo-Song bifurcation theorem [36], we have shown that our model always undergoes a transcritical bifurcation when the control reproduction number is equal to one.

To analyze the impact of case detection and treatment on our model, we perform a sensitivity analysis on the control reproduction number of our model. We have shown that the mortality rate always has a significant impact on the control reproduction number, and increasing this parameter will reduce the control reproduction number. We also find that increasing case detection and its efficiency can reduce the control reproduction number significantly. Furthermore, we notice that the efficiency (successful probability) of the first dose treatment is more significant in reducing the control reproduction number compared to the second dose treatment. These results indicate the importance of case detection and increasing the efficiency of early treatment in an effort to prevent and treat lymphatic filariasis cases.

In this paper, we have shown the promising potential result of the implementation of case detection and intensive treatment to control lymphatic filariasis. A proper combination of these two interventions can be used to optimize the controlling effort for lymphatic filariasis eradication. We expect that these results can be a good aid in controlling lymphatic filariasis transmission.

ACKNOWLEDGEMENTS

We thank all the reviewers for their valuable comments and suggestions. This research is funded by Universitas Indonesia with PUTI 2023 research grant scheme (ID: NKB-470/UN2.RST/HKP.05.00/2023).

APPENDIX

Appendix 1. Expression of B_0 and B_1.

$$B_0 = \mu_v^2 N_h^2 \mu_h (\mu_h + \delta_2)(\mu_h + \eta_c)(\mu_h + \alpha + \delta_1)(\alpha + \mu_h + \eta_a)(\eta_t + 1),$$

$$B_1 = \Lambda_h \Lambda_v \beta_v (\delta_1 (\mu_h + \delta_2)((1-q)\eta_t \xi_c + \xi_t (\mu_h + \eta_c)) + \delta_2 \alpha (\alpha + \mu_h + \eta_a)((1-p)(1-q)\eta_t \xi_c + (1-p)\xi_t (\mu_h + \eta_c)).$$

Appendix 2. Expression of $p_1, p_2, q_1,$ and q_2.

$$p_1 = q_1 = -\mu_v^2 N_h((\eta_t + \mu_h)(\delta_2 + \mu_h)(\eta_c + \mu_h)(\alpha^2 + (\eta_a + 2\mu_h + \delta_1)\alpha + (\delta_1 + \mu_h)(\eta_a + \mu_h)),$$

$$p_2 = q_2 = \Lambda_v \beta_v ((1-p)((1-q)\eta_t \xi_c + \xi_t(\mu_h + \eta_c))\delta_2 \alpha^2 + ((1-q)\eta_t \xi_c + \xi_t(\mu_h + \eta_c))((\delta_2 + \mu_h)\delta_1 + (1-p)(\mu_h + \eta_a)\delta_2 \alpha + \delta_1(\delta_2 + \mu_h)(\mu_h + \eta_t)(\eta_a \xi_c + \eta_c + \mu_h)).$$

Appendix 3. Right eigenvector of Model 1.

$$w_1 = \frac{w_{11}}{w_{12}}, \quad w_2 = \frac{\delta_2 + \mu_h}{\alpha} w_3, \quad w_3 = w_3, \quad w_4 = \frac{(\delta_2 + \mu_h)\delta_1}{\alpha(\eta_a + \alpha + \mu_h)} w_3,$$

$$w_5 = \frac{(\mu_h + \delta_2)\delta_1 + \delta_2(1-p)(\alpha + \mu_h + \eta_a)}{(\mu_h + \eta_t)(\alpha + \mu_h + \eta_a)} w_3,$$

$$w_6 = \frac{w_{61}}{w_{62}} w_3, \quad w_7 = \frac{w_{71}}{w_{72}} w_3, \quad w_8 = \frac{w_{81}}{w_{82}} w_3, \quad w_9 = \frac{w_{91}}{w_{92}} w_3,$$

with

$$w_{11} = (\delta_2 + \mu_h)(((1-q)\eta_t + \eta_c \mu_h)\alpha + (\mu_h + \eta_t)(\mu_h + \eta_a + \eta_c)\omega + (\mu_h + \eta_t)(\eta_c + mu_h)(\alpha + \eta_a + \mu_h)\delta_1 + (\alpha + \eta_a + \mu_h)((1-p)((1-q)\eta_t + \eta_c + \mu_h)\omega + (\eta_c + \mu_h)(\mu_h + \eta_t)\alpha + (\mu_h + \omega)(\mu_h + \eta_t)(\eta_c + \mu_h)(\alpha + \mu_h + \delta_2),$$

$$w_{12} = w_{72} = \alpha(\mu_h + \omega)(\mu_h + \eta_t)(\mu_h + \eta_c)(\alpha + \mu_h + \eta_a),$$

$$w_{61} = \delta_1(\mu_h + \delta_2)(\eta_a(\mu_h + \eta_t) + (1-q)\alpha\eta_t) + \alpha\eta_t\delta_2(1-q)(1-p)(\alpha + \mu_h + \eta_a),$$

$$w_{62} = \alpha(\mu_h + \eta_t)(\mu_h + \eta_c)(\alpha + \mu_h + \eta_a),$$

$$w_{71} = \delta_1(\eta_t(\mu_h q + \eta_c)\alpha + \eta_a \eta_C(\mu_h + \eta_t))(\mu_h + \delta_2) + \alpha\delta_2(((1-q)\eta_t + \mu_h + \eta_c)p\mu_h + (\mu_h q + \eta_c)(\alpha + \mu_h + \eta_a)\eta_t),$$

$$w_{81} = w_{91} = -\Lambda_v \beta_v ((1-p)((1-q)\eta_t \xi_c + \xi_t(\mu_h + \eta_c))\delta_2 \alpha^2$$
$$+ ((1-q)\eta_t \xi_c + \xi_t(\mu_h + \eta_c))((\delta_2 + \mu_h)\delta_1$$
$$+ (1-p)(\mu_h + \eta_a)\delta_2 \alpha + \delta_1(\delta_2 + \mu_h)(\mu_h + \eta_t)(\eta_a \xi_c + \eta_c + \mu_h)),$$
$$w_{82} = w_{92} = \alpha \mu_v^2 N_h((\mu_h + \eta_t)(\mu_h + \eta_c)(\alpha + \mu_h + \eta_a)).$$

Appendix 4. Left eigenvector of Model 1.

$$v_1 = 0, \quad v_2 = \frac{v_{21}}{v_{22}}, \quad v_3 = \frac{\delta_2(p-1)((q-1)\eta_t \xi_c - \eta_c \xi_t - \mu_h \xi_t)}{\xi_c(\eta_t + \mu_h)(\delta_2 + \mu_h)} v_6,$$
$$v_4 = \frac{((1-q)\,\alpha\,\eta_t + \eta_a\,(\mu_h + \eta_t))\,\xi_c + (\mu_h + \eta_c)\,(\alpha\,\xi_t + \eta_t + \mu_h)}{\xi_c\,(\mu_h + \eta_t)\,(\alpha + \mu_h + \eta_a)} v_6,$$
$$v_5 = \frac{(1-q)\eta_t \xi_c + \eta_c \xi_t + \mu_h \xi_t}{\xi_c(\eta_t + \mu_h)} v_6,$$
$$v_6 = v_6, \quad v_7 = 0, \quad v_8 = 0, \quad v_9 = \frac{(\eta_c + \mu_h)\mu_v N_h}{\beta_v \Lambda_v \xi_c} v_6,$$

with

$$v_{21} = (1-p)\,((1-q)\,\eta_t \xi_c + \xi_t\,(\mu_h + \eta_c))\,\delta_2 \alpha^2 + ((1-q)\,\eta_t \xi_c + \xi_t\,(\mu_h + \eta_c))$$
$$((\delta_2 + \mu_h)\,\delta_1 + (1-p)\,\delta_2\,(\mu_h + \eta_a))\,\alpha + \delta_1\,(\delta_2 + \mu_h)\,(\mu_h + \eta_t)\,(\eta_a \xi_c + \eta_c + \mu_h)\,,$$
$$v_{22} = (\delta_2 + \mu_h)\,(\mu_h + \eta_t)\,(\alpha + \mu_h + \delta_1)\,(\alpha + \eta_a + \mu_h)\,.$$

CONFLICT OF INTERESTS

The authors declare that there is no conflict of interests.

REFERENCES

[1] M. Masrizal, Penyakit filariasis, Jurnal Kesehatan Masyarakat Andalas. 7 (2012), 32-38. https://doi.org/10.24893/jkma.v7i1.105.

[2] G. Meliyanie, D. Andiarsa, Program eliminasi lymphatic filariasis di Indonesia, JHECDs: J. Health Epidemiol. Commun. Dis. 3 (2017), 63-70.

[3] Y. Otsuji, History, epidemiology and control of filariasis, Trop. Med. Health. 39 (2011), 3-13.

[4] A.A. Arsin, Epidemiologi filariasis di Indonesia, Masagena Press, Makassar, (2016).

[5] World Health Organization (WHO), Lymphatic filariasis, (2022). https://www.who.int/news-room/fact-sheets/detail/lymphatic-filariasis.

[6] Kementerian Kesehatan Republik Indonesia, Profil Kesehatan Indonesia Tahun 2019, Kementerian Kesehatan, Jakarta, (2019).

[7] World Health Organization (WHO), Vector-borne diseases, (2020). https://www.who.int/news-room/fact-sheets/detail/vector-borne-diseases.

[8] World Health Organization (WHO), Screening programmes: a short guide, (2020). https://apps.who.int/iris/bitstream/handle/10665/330829/9789289054782-eng.pdf.

[9] Coalition for operational research on neglected tropical disease (COR-NTD), filariasis test strip, (2016). https://www.cor-ntd.org/resources/filariasis-test-strip-fts-bench-aid.

[10] K. Gass, M.V.E. Beau de Rochars, D. Boakye, et al. A multicenter evaluation of diagnostic tools to define endpoints for programs to eliminate bancroftian filariasis, PLoS Negl Trop Dis. 6 (2012), e1479. https://doi.org/10.1371/journal.pntd.0001479.

[11] World Health Organization (WHO), Responding to failed transmission assessment surveys, Report of an Ad Hoc Meeting, (2016). https://www.who.int/publications-detail-redirect/9789241511292.

[12] D. Aldila, Dynamical analysis on a malaria model with relapse preventive treatment and saturated fumigation, Comput. Math. Methods Med. 2022 (2022), 1135452. https://doi.org/10.1155/2022/1135452.

[13] B.D. Handari, R.A. Ramadhani, C.W. Chukwu, et al. An optimal control model to understand the potential impact of the new vaccine and transmission-blocking drugs for malaria: a case study in Papua and West Papua, Indonesia, Vaccines. 10 (2022), 1174. https://doi.org/10.3390/vaccines10081174.

[14] H. Tasman, D. Aldila, P.A. Dumbela, et al. Assessing the impact of relapse, reinfection and recrudescence on malaria eradication policy: a bifurcation and optimal control analysis, TropicalMed. 7 (2022), 263. https://doi.org/10.3390/tropicalmed7100263.

[15] D. Aldila, Optimal control for dengue eradication program under the media awareness effect, Int. J. Nonlinear Sci. Numer. Simul. 24 (2023), 95-122. https://doi.org/10.1515/ijnsns-2020-0142.

[16] D. Aldila, M.Z. Ndii, N. Anggriani, et al. Impact of social awareness, case detection, and hospital capacity on dengue eradication in Jakarta: a mathematical model approach, Alexandria Eng. J. 64 (2023), 691-707. https://doi.org/10.1016/j.aej.2022.11.032.

[17] D. Aldila, J.P. Chavez, K.P. Wijaya, et al. A tuberculosis epidemic model as a proxy for the assessment of the novel $M72/AS01_E$ vaccine, Commun. Nonlinear Sci. Numer. Simul. 120 (2023), 107162. https://doi.org/10.1016/j.cnsns.2023.107162.

[18] D. Aldila, A. Islamilova, S.H.A. Khosnaw, et al. Forward bifurcation with hysteresis phenomena from atherosclerosis mathematical model, Commun. Biomath. Sci. 4 (2021), 125-137. https://doi.org/10.5614/cbms.2021.4.2.4.

[19] D. Aldila, M. Angelina, Optimal control problem and backward bifurcation on malaria transmission with vector bias, Heliyon. 7 (2021), e06824. https://doi.org/10.1016/j.heliyon.2021.e06824.

[20] D. Aldila, B.D. Handari, A. Widyah, et al. Strategies of optimal control for HIV spreads prevention with health campaign, Commun. Math. Biol. Neurosci. 2020 (2020), 7. https://doi.org/10.28919/cmbn/4332.

[21] A. K., N. Anggriani, Lymphatic filariasis transmission and control: a mathematical modelling approach, in: A. Rodriguez-Morales (Ed.), Current Topics in Tropical Medicine, InTech, 2012. https://doi.org/10.5772/36121.

[22] A.M. Fuady, E. Soewono, N. Nuraini, et al. A mass treatment model for endemic reduction of filaria disease with pre-testing, in: Bandung, Indonesia, 2012: pp. 241-245. https://doi.org/10.1063/1.4724147.

[23] P.M. Mwamtobe, S.M. Simelane, S. Abelman, et al. Mathematical analysis of a lymphatic filariasis model with quarantine and treatment, BMC Public Health. 17 (2017), 265. https://doi.org/10.1186/s12889-017-4160-8.

[24] P.K.N. Salonga, V.M.P. Mendoza, R.G. Mendoza, et al. A mathematical model of the dynamics of lymphatic filariasis in Caraga Region, the Philippines, R. Soc. Open Sci. 8 (2021), 201965. https://doi.org/10.1098/rsos.201965.

[25] A. K. Supriatna, H. Serviana, E. Soewono, A mathematical model to investigate the long-term effects of the lymphatic filariasis medical treatment in Jati Sampurna, West Java, ITB J. Sci. 41 (2009), 1-14. https://doi.org/10.5614/itbj.sci.2009.41.1.1.

[26] Y. Cheng, X. Wang, Q. Pan, et al. Modeling the parasitic filariasis spread by mosquito in periodic environment, Comput. Math. Methods Med. 2017 (2017), 4567452. https://doi.org/10.1155/2017/4567452.

[27] E. Michael, M.N. Malecela-Lazaro, P.E. Simonsen, et al. Mathematical modelling and the control of lymphatic filariasis, Lancet Infect. Dis. 4 (2004), 223-234. https://doi.org/10.1016/s1473-3099(04)00973-9.

[28] F.A. Oguntolu, G. Bolarin, O.J. Peter, et al. Mathematical model for the control of lymphatic filariasis transmission dynamics, Commun. Math. Biol. Neurosci. 2021 (2021), 17. https://doi.org/10.28919/cmbn/5307.

[29] P. Jambulingam, S. Subramanian, S.J. de Vlas, et al. Mathematical modelling of lymphatic filariasis elimination programmes in India: required duration of mass drug administration and post-treatment level of infection indicators, Parasites Vectors. 9 (2016), 501. https://doi.org/10.1186/s13071-016-1768-y.

[30] E. Michael, M.N. Malecela-Lazaro, C. Kabali, et al. Mathematical models and lymphatic filariasis control: endpoints and optimal interventions, Trends Parasitol. 22 (2006), 226-233. https://doi.org/10.1016/j.pt.2006.03.005.

[31] S.M. Simelane, P.M. Mwamtobe, S. Abelman, et al. A mathematical model for the transmission dynamics of lymphatic filariasis with intervention strategies, Acta Biotheor. 68 (2019), 297-320. https://doi.org/10.1007/s10441-019-09370-y.

[32] H. Tasman, T. Supali, A.K. Supriatna, et al. A mathematical model for long-term effect of diethylcarbamazine-albendazole mass drug administration on lymphatic filariasis, AIP Conf. Proc. 1651 (2015), 138-146. https://doi.org/10.1063/1.4914445.

[33] D. Aldila, T. Windyhani, Backward bifurcation emerging from a mathematical model of African animal trypanosomiasis disease in white rhino populations, J. Math. Fund. Sci. 54 (2022), 151-189. https://doi.org/10.5614/j.math.fund.sci.2022.54.1.9.

[34] O. Diekmann, J.A.P. Heesterbeek, M.G. Roberts, The construction of next-generation matrices for compartmental epidemic models, J. R. Soc. Interface. 7 (2009), 873-885. https://doi.org/10.1098/rsif.2009.0386.

[35] P. van den Driessche, J. Watmough, A simple SIS epidemic model with a backward bifurcation, J. Math. Biol. 40 (2000), 525-540. https://doi.org/10.1007/s002850000032.

[36] M. Martcheva, An introduction to mathematical epidemiology, Springer, New York, 2015. https://doi.org/10.1007/978-1-4899-7612-3.

[37] W.E. Boyce, R.C. DiPrima, Elementary differential equations and boundary value problems, John Wiley and Sons, New York, (2001).

[38] J.H.F. Remme, P. Feenstra, P.R. Lever, et al. Tropical diseases targeted for elimination: chagas disease, lymphatic filariasis, onchocerciasis, and leprosy. In: D.T. Jamison, J.G. Breman, A.R. Measham, et al. (eds). Disease Control Priorities in Developing Countries. 2nd edition. Washington (DC): The International Bank for Reconstruction and Development, The World Bank; 2006.

[39] M.A. Dorkenoo, R. Bronzan, D. Yehadji, et al. Surveillance for lymphatic filariasis after stopping mass drug administration in endemic districts of Togo, 2010–2015, Parasites Vectors. 11 (2018), 244. https://doi.org/10.1186/s13071-018-2843-3.

[40] S. Rojanapanus, T. Toothong, P. Boondej, et al. How Thailand eliminated lymphatic filariasis as a public health problem, Infect. Dis. Poverty. 8 (2019), 38. https://doi.org/10.1186/s40249-019-0549-1.